

Structure-Function Analysis of the Coxsackievirus Protein 3A

IDENTIFICATION OF RESIDUES IMPORTANT FOR DIMERIZATION, VIRAL RNA REPLICATION, AND TRANSPORT INHIBITION*[‡]

Received for publication, February 6, 2006, and in revised form, July 18, 2006. Published, JBC Papers in Press, July 25, 2006, DOI 10.1074/jbc.M601122200

Els Wessels[‡], Richard A. Notebaart[§], Daniël Duijsings[‡], Kjerstin Lanke[‡], Bart Vergeer[‡], Willem J. G. Melchers[‡], and Frank J. M. van Kuppeveld^{‡1}

From the [‡]Department of Medical Microbiology, Radboud University Nijmegen Medical Centre, Nijmegen Centre for Molecular Life Sciences, 6500 HB Nijmegen, The Netherlands and the [§]Center for Molecular and Biomolecular Informatics, University of Nijmegen, 6500 GL Nijmegen, The Netherlands

The coxsackievirus B3 3A protein forms homodimers and plays important roles in both viral RNA (vRNA) replication and the viral inhibition of intracellular protein transport. The molecular determinants that are required for each of these functions are yet poorly understood. Based on the NMR structure of the closely related poliovirus 3A protein, a molecular model of the coxsackievirus B3 3A protein was constructed. Using this structural model, specific mutants were designed to study the structure–function relationship of 3A. The mutants were tested for their capacity to dimerize, support vRNA replication, and block protein transport. A hydrophobic interaction between the monomers and an intermolecular salt bridge were identified as major determinants required for dimerization. We show that dimerization is important for both efficient vRNA replication and inhibition of protein transport. In addition, determinants were identified that were not required for dimerization but that were essential for either one of the biological functions of 3A. The combination of the *in silico* and *in vivo* results obtained in this study provides important insights in both the structural and functional aspects of 3A.

Enteroviruses are small RNA viruses that belong to the family of the Picornaviridae. The enteroviruses are divided into several species, e.g. poliovirus (PV),² human enterovirus A (HEV-A), human enterovirus B (HEV-B, which includes coxsackieviruses B (CVB)), human enterovirus C (HEV-C), and human enterovirus D (HEV-D). The enterovirus genome encodes a large

polyprotein that is divided into P1, P2, and P3 regions and is processed by virally encoded proteases to yield the capsid proteins and the nonstructural proteins, as well as some relatively stable precursor proteins (1, 2). The nonstructural proteins are involved in viral RNA (vRNA) replication and account for the virus-induced alterations in host cell metabolism and structure. These alterations serve to create an environment that is suitable for efficient vRNA replication and/or to suppress anti-viral host cell responses.

Enteroviruses are nonenveloped, cytolitic viruses that replicate on secretory pathway-derived membrane vesicles. These viruses do not need an intact secretory pathway to release their virus progeny. Instead, the viral nonstructural proteins 2B and 3A have been shown to inhibit protein transport through the secretory pathway (3). 3A inhibits protein transport between the endoplasmic reticulum and Golgi (4, 5), whereas the step inhibited by the 2B protein is presently unknown. The inhibition of protein transport by 3A is not essential for viral replication in cell culture (4, 5) but has been proposed to have a function in evasion of innate and acquired immune responses and the extrinsic apoptotic pathway (6–8).

In addition to inhibiting protein transport, the 3A protein is involved in multiple steps in the process of vRNA replication. Several mutations in 3A were shown to cause defects in vRNA synthesis (9–12). However, the exact role of 3A, or its precursor 3AB, is not completely understood. 3AB is thought to deliver VPg (3B), the protein primer for RNA synthesis, to the replication complex where vRNA synthesis takes place (13). In addition, several other activities have been suggested for 3AB: (i) stimulation of autoprocessing of the 3CD^{Pro} precursor protein to produce the 3C^{Pro} protease and the 3D^{Pol} polymerase (14), (ii) stimulation of the polymerase activity of 3D^{Pol} (15, 16), (iii) stimulation of the binding of 3CD^{Pro} to the vRNA (17), and (iv) mediating binding of 3D^{Pol} to membranes (18).

3A is a small protein (87–89 aa) that is associated to membranes via its C-terminal hydrophobic domain (19). The structure of the soluble N terminus (aa 1–59) of PV 3A has been resolved by NMR (20). PV 3A was shown to form a homodimer. Each monomer consists of two amphipathic α -helices (aa 23–29 and 32–41), which are bent 180° to form a helical hairpin, flanked by unstructured N and C termini. To gain insight into the structure–function relationship of the CVB3 3A protein, we generated a molecular model of this protein using the PV 3A structure as template. We used this model to design

* This work was supported in part by Netherlands Organization for Scientific Research Grant NWO-VIDI-917.46.305, a grant from the M. W. Beijerinck Virology Fund from the Royal Netherlands Academy of Sciences, and European Communities Grant INTAS 2012. The costs of publication of this article were defrayed in part by the payment of page charges. This article must therefore be hereby marked “advertisement” in accordance with 18 U.S.C. Section 1734 solely to indicate this fact.

[‡] The on-line version of this article (available at <http://www.jbc.org>) contains supplemental Table S1.

¹ To whom correspondence should be addressed: Dept. of Medical Microbiology, Radboud University Nijmegen Medical Centre, Nijmegen Centre for Molecular Life Sciences, P.O. Box 9101, 6500 HB Nijmegen, The Netherlands. Tel.: 31-24-3617574; Fax: 31-24-3614666; E-mail: f.vankuppeveld@ncmls.ru.nl.

² The abbreviations used are: PV, poliovirus; CVB3, coxsackievirus B3; vRNA, viral RNA; HEV, human enterovirus; aa, amino acid(s); wt, wild type; BGM, buffalo green monkey; MEM, minimal essential medium; GuHCl, guanidine hydrochloride; CND, conserved N-terminal domain; EGFP, enhanced green fluorescent protein.

mutants and tested them for their ability to dimerize, inhibit protein transport, and support vRNA replication. Our data show that dimerization is important for efficient functioning of 3A. In addition, we identified determinants in 3A that do not affect dimerization but that do affect the ability to inhibit protein transport or to support vRNA replication.

EXPERIMENTAL PROCEDURES

Cells

CVB3 (wild type (wt) and mutants) were grown in buffalo green monkey (BGM) kidney cells because this cell line allows efficient and high level CVB3 replication. BGM cells were grown in minimal essential medium (MEM) (Invitrogen) supplemented with 10% fetal bovine serum. COS-1 cells were grown in Dulbecco's modified Eagle's medium (Invitrogen) supplemented with 10% fetal bovine serum. The cells were grown at 37 °C in a 5% CO₂ incubator.

Site-directed Mutagenesis

In vitro mutagenesis was performed with single-stranded DNA generated from a subgenomic pALTER phagemid construct that contained the XhoI (nucleotide 2014) to SalI (nucleotide 7438) fragment of CVB3, using the Altered Sites *in vitro* mutagenesis system according to the recommendations of the manufacturer (Promega). The following synthetic oligonucleotides were used to introduce unique restriction sites without modifying the aa sequence at positions 5020 (at the end of the 2C coding region) and 5169 (in the middle of the 3A coding region): 5'-TGG TCC CTG GAA CAA GGC CTC AAG CGT GGT-3' (primer p388.16, StuI site underlined) and 5'-GGA GTT GAT CTC CGG AAC CAA CCA-3' (primer 388.17, BseAI site underlined), respectively. pALTER clones containing either the BseAI site (pALTER-3A[BseAI]) or both the StuI and BseAI sites (pALTER-2C[StuI]/3A[BseAI]) were generated.

Plasmids

pEGFP-3A Mutants—For the construction of pEGFP-3A(BseAI), the 3A coding sequence including the BseAI restriction site was amplified from pALTER-3A(BseAI). The forward primer introduced XhoI and EcoICRI sites and amplified the 3A coding sequence without start codon in frame with EGFP (p416.2: 5'-GGG GGC TCG AGT GGA GCT CTG TTC CAG GGA CCA CCA-3', XhoI and EcoICRI sites underlined), and the reverse primer introduced a stop codon followed by a BamHI restriction site (p120-5, 5'-GGG GGG GGA TCC CTA TTG AAA ACC CGC AAA GAG-3', BamHI site underlined). The PCR product was cloned in pEGFP-C2 (Clontech) using XhoI and BamHI. The mutant 3A proteins were generated by PCR amplification using primers that introduced specific mutations and in some cases silent mutations to introduce extra restriction sites for rapid identification of mutations (see supplemental Table S1). The PCR products were cloned in pEGFP-3A(BseAI) using either XhoI and Scal restriction sites (3A-R6A/E7A/I8A/K9A/I10A, 3A-R6A, 3A-E7A, 3A-I8A, 3A-K9A, 3A-I10A, 3A-D24A, 3A-L25A/L26A, and 3A-S28A) or XhoI and BseAI restriction sites (3A-Y37A). The nucleotide

sequence of the mutant 3A proteins was verified by sequence analysis. The second site suppressor mutations that were found after RNA transfection were cloned from the p53CB3/T7 mutant clones into the EGFP-3A(BseAI) clone using Bst1107I and BseAI.

p53CB3/T7 Mutants—The CVB3 infectious cDNA clone used in this study was p53CB3/T7 (5), which contains a full-length cDNA of CVB3 (strain Nancy) behind a T7 RNA polymerase promoter. For the construction of p53CB3/T7-StuI(5020)/BseAI(5169), the fragment containing the extra restriction sites was cut from pALTER-2C(StuI)/3A(BseAI) using the enzymes XbaI and BstEII and cloned in p53CB3/T7. p53CB3/T7 constructs containing mutant 3A sequences were generated by cloning mutant 3A sequences from pEGFP-3A (using BseAI and the blunt site EcoICRI) in p53CB3/T7-StuI(5020)/BseAI(5169), from which 3A was removed by cutting with StuI (blunt) and BseAI. In case a new and/or extra mutation was found in the vRNA after RNA transfection, p53CB3/T7 constructs containing the mutant 3A sequences were generated by PCR. First RNA was isolated from the virus using the GenElute Mammalian Total RNA Miniprep Kit (Sigma) according to the instructions of the manufacturer. Reverse transcription-PCR was performed with primer 5'-GAA CTC AAA GTC GAC TTA TTG CAC TTT TGC TTG CCT-3' (p120.2, reverse primer 3B) via standard procedures. The reverse transcription-PCR product was used as template for PCR using primers 5'-CAG GTC AGA TAC TCT CTA **GAC ATG**-3' (p305.10, forward primer containing a XbaI site (bold) in 2C) and 5'-GGA GTT GAT CTC **CGG AAC** CAA CCA-3' (p388.17, reverse primer introducing a BseAI site (bold) at position 46 in 3A). The PCR product was cloned into p53CB3/T7(StuI/BseAI) using XbaI and BseAI. The nucleotide sequence of the mutant 3A sequences was verified by sequence analysis.

pRib-CB3-LUC—Plasmid pRib-CB3-LUC, which contains the firefly luciferase gene in place of the P1 capsid coding region, was described previously (21). pRib-CB3-LUC-3A mutant clones were generated from p53CB3/T7-3A mutants using the restriction enzymes BssHIII and PvuI.

Mammalian Two-hybrid Plasmids—pACT, pBIND, and pG5luc plasmids were obtained from the Checkmate mammalian two-hybrid system (Promega). pACT-3A and pBIND-3A were described previously (5). To obtain pACT and pBIND-3A mutant plasmids, the wt 3A sequence was replaced by mutant 3A sequences using the enzymes Bst1107I and BamHI.

pC-A1PI-EYFP-S-EGFP-3A Mutants

pC-A1PI-EYFP-S-EGFP-3A was described previously (5). pC-A1PI-EYFP-S-EGFP-3A mutants were obtained by replacing the EGFP-3A wt sequence for EGFP-3A mutant sequences using restriction enzymes AgeI and XbaI.

Mammalian Two-hybrid Analysis

COS-1 cells grown in 24-well plates were transfected with a total of 1 μg of plasmid DNA (1:1:1 mix of the pACT:pBIND:pG5luc plasmids) using FuGENE 6 reagent according to the instructions of the manufacturer (Roche Applied Science). At 48 h post-transfection, the cells were lysed, and both the firefly

Structure-Function Analysis of CVB3 3A

luciferase and *Renilla* luciferase enzyme activities were measured from the same cell lysate using a dual luciferase reporter assay system (Promega), as described previously (22). Analysis of the *Renilla* luciferase activity, which is encoded by the pBIND plasmid and which allows monitoring of the transfection efficiency, revealed no gross differences in transfection efficiency among the different samples. For all of the mutants the luciferase activities of three sample combinations were measured: (i) the pACT-3A and pBIND-3A fusion proteins, (ii) the pACT-3A fusion protein with unfused pBIND, and (iii) the pBIND-3A fusion protein with unfused pACT. For all luciferase activities the background luciferase activity, which was produced upon expression of unfused pACT and pBIND proteins, was subtracted. The firefly luciferase activity produced in cells expressing the pACT-3A fusion proteins and unfused pBIND was always much higher than that of the pBIND-3A fusion proteins and unfused pACT. Dimerization efficiency was expressed as the ratio between the firefly luciferase activity measured in cells coexpressing pACT and pBIND fusion proteins *versus* that measured in cells coexpressing pACT fusion proteins and unfused pBIND. This ratio was set at 100% for wild type 3A. Western blot analysis using a polyclonal antibody raised against recombinant 3A (1–60) was performed to monitor expression of the pACT-3A and pBIND-3A fusion proteins.

A1PI Secretion Assay

The A1PI secretion assay was performed as described previously (5). In short, BGM cells were transfected with 2 μ g of plasmid DNA/well and at 20 h after transfection incubated in MEM lacking methionine (Sigma) for 30 min at 37 °C. The proteins were pulse-labeled with [³⁵S]methionine for 30 min at 37 °C and washed twice with phosphate-buffered saline, after which 800 μ l of fresh serum-free MEM was added. After 2 h of chase, the medium was collected, and the cells were lysed in 1 ml of lysis buffer. Anti-EGFP rabbit polyclonal antiserum (1:1,000) was added to the cell lysate and culture medium, and the antibody-protein complexes were collected with protein A-Sepharose (Amersham Biosciences), washed, and precipitated. The samples were resuspended in 25 μ l of Laemmli sample buffer, boiled for 5 min, and analyzed by SDS-PAGE. The amount of radiolabeled A1PI-EYFP in the cell fraction, and medium fraction was quantified using a phosphorimaging device (Bio-Rad Multi-Analyst version 1.0.1). The amount of A1PI in the medium fraction was determined as a percentage of the total amount of A1PI and compared with that of control cells (for which the value was normalized to 100% A1PI secretion). Western blot analysis showed that all mutant 3A proteins were efficiently expressed (data not shown).

Analysis of Virus Growth

Plasmids were linearized with MluI, purified, and transcribed *in vitro* by T7 RNA polymerase as described previously (23). The RNA transcripts were checked by agarose gel electrophoresis. BGM cells grown in 25-cm² flasks to subconfluency were transfected with 2.5 μ g of RNA transcripts using DEAE-dextran as described previously (23). After transfection, the cells were grown at 37 °C. When virus growth was observed, the

cultures were incubated until the cytopathic effect was complete. In case no cytopathic effect was observed after 5 days, the cultures were subjected to three successive cycles of freezing and thawing, and 200 μ l was passaged to fresh BGM monolayer cells, which were grown at 37 °C for another 5 days.

Analysis of vRNA Replication

BGM cells grown in 6-well plates to subconfluency were transfected with 1 μ g of T7 RNA polymerase generated RNA transcripts of MluI-linearized pRib-CB3/T7-LUC plasmids as described above. At 8 h post-transfection, the cells were lysed, and luciferase activity was assayed as described previously (23). Transfected cells were grown in the absence or presence of guanidine hydrochloride (GuHCl), an inhibitor of enterovirus replication that is used to determine the luciferase levels in the absence of replication (under this condition, luciferase production reflects translation of the transfected replicon RNA). The level of replication is expressed as the ratio of luciferase produced in the presence or absence of GuHCl.

Sequence Analysis of vRNA

RNA was isolated from virus suspensions and reverse transcribed as described previously (23). The 3A coding region was amplified by PCR using SuperTaqDNA polymerase (HT Biotechnology) and subjected to sequence analysis.

Single-cycle Growth Analysis

BGM cell grown in flat-bottomed tubes to subconfluency were infected with virus at a multiplicity of infection of 5 TCID₅₀ (tissue culture infective dose) for 30 min at 37 °C. The cells were washed three times with phosphate-buffered saline, supplied with MEM, grown at 37 °C, and harvested at the indicated times. The viruses were released by three cycles of freezing and thawing, and virus titers were determined by end point titration as described previously (5).

Plaque Assays

Plaque assays were performed as described in Ref. 24. In short, BGM cells were grown in 6-well plates to subconfluency and infected with serial dilutions of CVB3 wt or mutants. At 30 min post-infection, the virus was replaced for M199 medium containing 0.5% agarose. The cells were incubated at 37 °C for 2 days, fixed, and stained with crystal violet.

Statistical Analysis

The data are presented as the mean values \pm S.E. The differences were tested for significance by Student's *t* test (Figs. 2, B and D, and 6B) or analysis of variance using Bonferroni's multiple comparison test (Figs. 2C; 3, B–E; 5, B–D; and 6C) using GraphPad Prism.

RESULTS

Molecular Model of the 3A Protein—We constructed a molecular model of the N-terminal 60 aa of CVB3 3A using the WHAT_IF software (Fig. 1A) (5, 25). In this program, the backbone of the protein model is derived from a structurally similar protein (that serves as a template), and side chains are replaced according to differences in sequence alignment (25). As a tem-

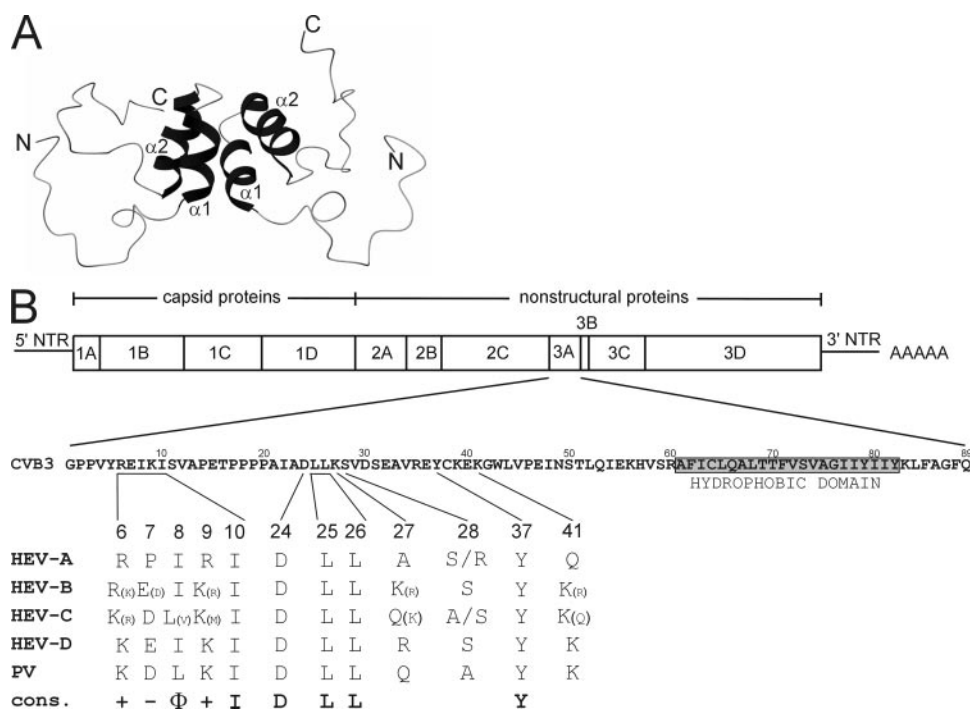


FIGURE 1. Putative model of the CVB3 3A protein and an alignment of several residues of the enterovirus 3A proteins. A, model of the homodimer formed by the N-terminal 60 aa of CVB3 3A. N, N terminus; C, C terminus; $\alpha 1$, first α -helix (aa 20–27); $\alpha 2$, second α -helix (aa 31–42). B, genome organization of CVB3. CVB3 contains a single open reading frame, flanked by a 5' and 3' nontranslated region (NTR) and a poly(A) tail. The four capsid proteins (1A, 1B, 1C, and 1D) and seven nonstructural proteins (2A, 2B, 2C, 3A, 3B, 3C, and 3D) are shown. The 3A protein of CVB3 is an 89-aa protein that contains a C-terminal hydrophobic domain (aa 61–82). An alignment of aa 6–10, 24–28, 37, and 41 of all enteroviruses sequenced to date is shown. The species names are shown in *bold*. *cons.*, consensus. Letter size indicates the prevalence of a specific residue in the species. +, positively charged aa; –, negatively charged aa; Φ , hydrophobic aa.

plate, we used sequence and structure information from the soluble N terminus of the PV 3A protein (aa 1–59), which has been resolved by NMR spectrometry (20). The conformation of replaced side chains was determined using the position-specific rotamer method, which is a component of the WHAT_IF software (26). Having 47% identity and an almost gapless alignment between the PV and CVB3 3A sequences, the two proteins were predicted to share a common fold. Subsequently, the CVB3 3A model was optimized using the YASARA NOVA force field package (27) and finally validated by WHAT_CHECK (28) (Fig. 1A). CVB3 3A was predicted to form a homodimer. Each monomer consists of two α -helices (aa 20–27 and 31–42) connected by a relatively large loop. For PV 3A, it was described that a conserved hydrophobic surface, which is mainly made up from residues in the central amphipathic α -helices, could form a dimer interface with the hydrophobic surface of the other molecule (20). For CVB3 3A, modeling identified various amino acids that could play a role in 3A homodimerization. These include (i) Ile²², Leu²⁵, Leu²⁶, Val²⁹, and Val³⁴, which were predicted to be involved in the hydrophobic packing of the homodimer; (ii) Asp²⁴ and Lys⁴¹, which were predicted to form an intermolecular salt bridge; and (iii) Ser²⁸ and Tyr³⁷, which were predicted to form an intermolecular hydrogen bond. Based on this model, we substituted individual residues, most of which were predicted to be involved in dimerization, for Ala residues to study their role in (i) homodimerization, (ii) inhibition of protein transport, and (iii) support of vRNA replication.

Leu²⁵ and Leu²⁶ Are Important for Dimerization, Inhibition of Protein Transport, and vRNA Replication—Firstly, we studied the role of Leu²⁵ and Leu²⁶, which are identical in all enteroviruses sequenced to date (Fig. 1B) and are predicted to be part of the hydrophobic packing (Fig. 2A). Mutations resulting in alanine substitutions of both residues were introduced into the 3A coding sequence. The resulting L25A/L26A mutant was tested in a mammalian two-hybrid assay for the effect of these substitutions on dimerization (Fig. 2B). The firefly luciferase activity, which represents the ability to form homodimers in this system (for a detailed description, see “Experimental Procedures” and legends to Fig. 2), was significantly reduced to ~25% of wt levels ($p < 0.05$). Thus, Leu²⁵ and Leu²⁶ are important for dimerization.

Second, we studied whether the L25A/L26A mutant was able to inhibit protein secretion. To test for this ability, we expressed 3A from a plasmid that contains a second expression cassette encoding the $\alpha 1$ protease inhibitor (A1PI) reporter protein. After expression, cell and medium fractions were analyzed for the amount of reporter protein present. The ratio of A1PI in medium *versus* cell fractions was used as a measure to represent the ability of 3A to inhibit protein secretion. The ratio in control cells (expressing EGFP and A1PI) was set at 100%. Whereas expression of wt 3A reduced secretion levels to ~30% of control cells, the L25A/L26A mutant was no longer able to inhibit secretion (Fig. 2C).

Third, we investigated whether Leu²⁵ and Leu²⁶ were important for the ability to support vRNA replication. To this end, the L25A/L26A mutations were introduced into an infectious cDNA clone of CVB3. RNA transcripts of this clone were transfected into BGM cells, but no viruses were obtained. *In vitro* translation reactions showed that the introduced substitutions did not induce obvious alterations in the processing pattern of viral proteins, suggesting that it is unlikely that the lack of virus growth is caused by disrupted polyprotein processing (data not shown). To investigate whether the lack of virus growth is due to a primary defect in vRNA replication, the mutations L25A/L26A were introduced into a pRib-CB3/T7-LUC subgenomic replicon. This replicon contains the luciferase gene in place of the P1 coding region. BGM cells were transfected with RNA transcripts of this clone and incubated in either the presence or absence of an inhibitor of enterovirus replication (GuHCl). At 8 h post-transfection, the cells were lysed, and luciferase

Structure-Function Analysis of CVB3 3A

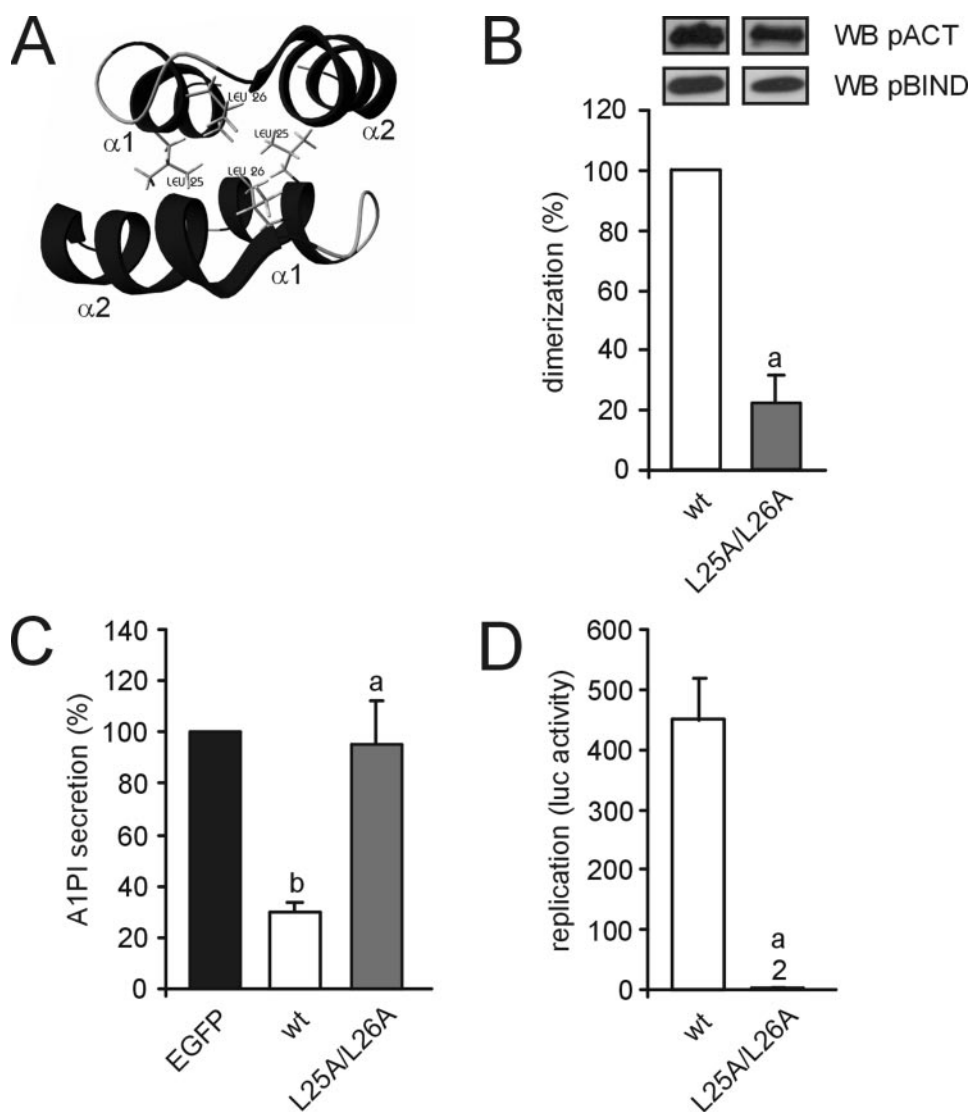


FIGURE 2. Leu²⁵ and Leu²⁶ are important for dimerization, inhibition of protein transport, and vRNA replication. *A*, structural model of the predicted hydrophobic packing in which Leu²⁵ and Leu²⁶ are depicted. *B*, homodimerization reactions of wt 3A and the L25A/L26A mutant expressed as fusion proteins to the HSV VP16 activation domain (*pACT*) or the yeast GAL4 DNA-binding domain (*pBIND*). At 48 h post-transfection the firefly luciferase production was assayed. Dimerization efficiency was expressed as the ratio between the firefly luciferase activity measured in cells coexpressing *pACT* and *pBIND* fusion proteins versus that measured in cells coexpressing *pACT* fusion proteins and unfused *pBIND*. This ratio was set at 100% for 3A wt, and the ratio of the mutant was compared with that of 3A wt of the same experiment (for details, see "Experimental Procedures"). The insets show the protein expression levels of the *pACT*-3A and *pBIND*-3A fusion proteins as detected by Western blot analysis (WB) with a polyclonal antibody against 3A. *C*, BGM cells were transfected with constructs expressing either EGFP, EGFP-3A wt, or EGFP-3A-L25A/L26A from an SV40 promoter and the A1PI-EYFP protein from a cytomegalovirus promoter. The amount of A1PI in the medium fraction was determined as the percentage of the total amount of A1PI and compared with that of control cells (for which the value was normalized to 100% A1PI secretion). *D*, effect of mutations L25A/L26A on vRNA replication. Mutations L25A/L26A were introduced in pRib-CB3/T7-LUC, and transcripts from these replicons were transfected into BGM cells. After 8 h of incubation in the presence or absence of 2 mM GuHCl, the cells were lysed, and the luciferase activity was measured. The luciferase activity measured in the presence of GuHCl represents the amount of protein translated from the input RNA, whereas the luciferase activity in the absence of GuHCl represents the amount of protein translated from input RNA plus replicated RNA. The level of vRNA replication is represented by the ratio of luciferase activities with or without GuHCl. The values depicted in the graphs of panels *B–D* represent the means \pm S.E. of at least three independent experiments. *a*, significantly different from 3A wt ($p < 0.05$); *b*, significantly different from A1PI secretion in control cells without 3A ($p < 0.05$).

expression was measured. The level of vRNA replication is represented by the ratio of luciferase activities with or without GuHCl. No detectable replication was observed with the L25A/L26A mutant (Fig. 2*D*). Together, our data show that the resi-

dues Leu²⁵ and Leu²⁶ are important for dimerization, inhibition of protein transport, and vRNA replication.

Asp²⁴ Is Important for Dimerization, Inhibition of Protein Transport, and vRNA Replication—Asp²⁴ is identical in all enteroviruses sequenced to date (Fig. 1*B*) and was predicted in the model to be important for dimerization of 3A by forming an intermolecular salt bridge with Lys⁴¹ (Fig. 3*A*). In addition to this intermolecular salt bridge, Asp²⁴ was also predicted to form an intramolecular salt bridge with Lys²⁷. Alanine substitution of Asp²⁴ abolished dimerization (Fig. 3*B*) and significantly reduced the ability of 3A to inhibit protein transport ($p < 0.05$) (Fig. 3*C*). To test whether this mutant could support virus growth, a total of 10 RNA transfections was performed. Virus growth was observed in nine cases (Fig. 4). Sequence analysis of the 3A coding regions of the obtained virus populations showed that mutation D24A caused a quasi-infectious phenotype (a definition that indicates that a mutation disrupts vRNA replication to such an extent that (pseudo)reversion mutations or second site suppressor mutations can arise, but no virus progeny can be observed harboring only the original mutation). In four of the nine cases, the virus had reverted back to wt. In three cases, the introduced mutation was retained in the virus, but second site suppressor mutations had occurred at position 41 (resulting in the genotypes D24A/K41N, D24A/K41Q, and D24A/K41E). In one case, a virus mixture was obtained in which a minor part of the population contained the introduced Asp-to-Ala substitution together with an additional Lys-to-Ile substitution at aa 27 (D24A/K27I), whereas the major part of the population contained the same Lys-to-Ile substitution, but the introduced Asp-to-Ala substitution at position 24 had reverted back to Asp (K27I) (Fig. 4). In the last case, the introduced Asp-to-Ala substitution had reverted back to Asp and was accompanied by a Lys-to-Ile substitution at position 27 (K27I). Together, these data show that Asp²⁴ is important for dimerization, inhibition of protein transport, and virus growth.

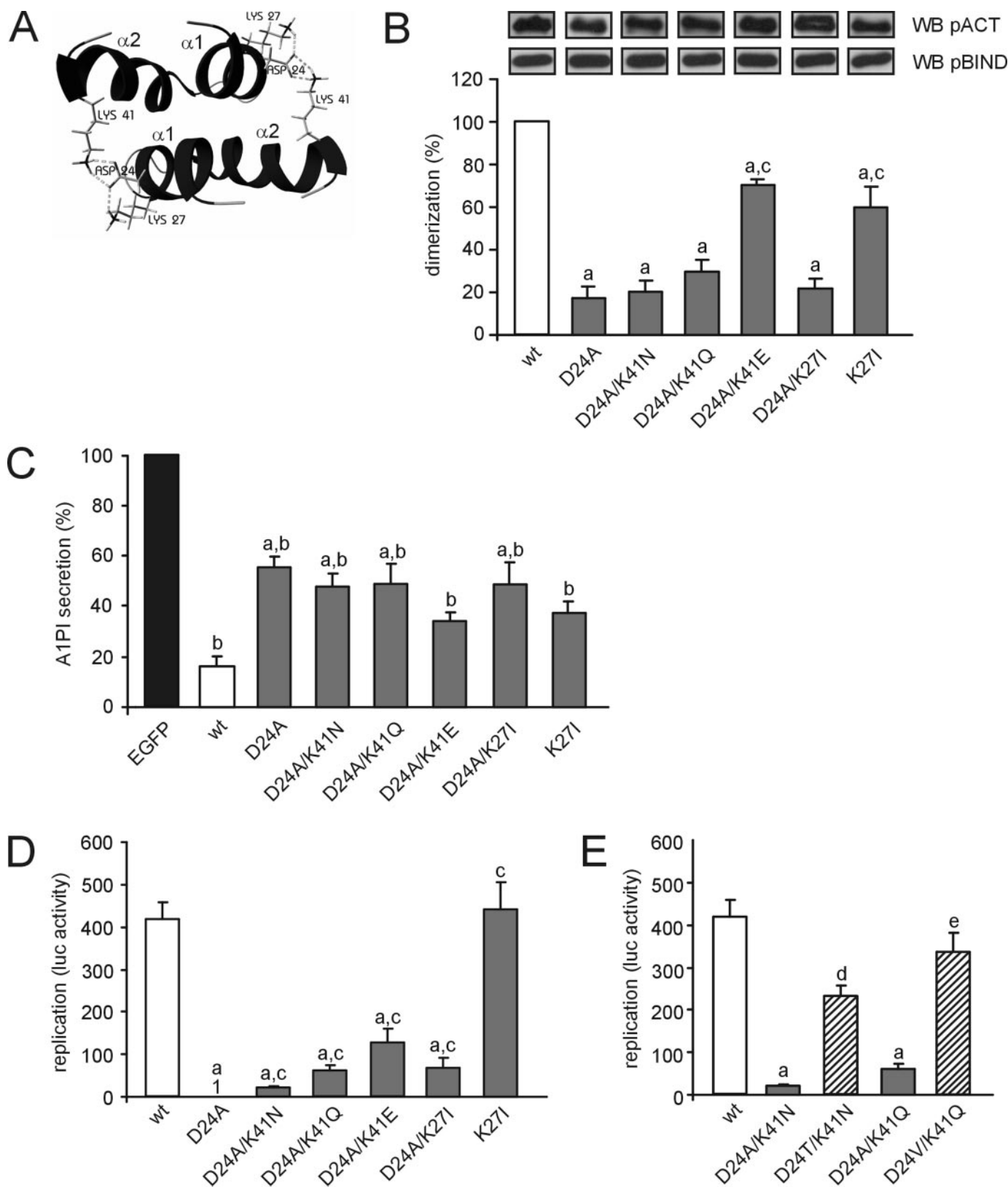


FIGURE 3. Asp²⁴ is important for dimerization, inhibition of protein transport, and virus growth, and several second site suppressor mutations rescue the effect of mutation 3A-D24A on virus growth. *A*, structural model of the predicted intermolecular salt bridge between Asp²⁴ and Lys⁴¹ and the intramolecular salt bridge between Asp²⁴ and Lys²⁷. *B*, effect of mutation D24A and its second site suppressor mutations on 3A dimerization. *C*, effect of mutation D24A and its second site suppressor mutations on the ability of 3A to inhibit protein transport. *D*, effect of D24A and its second site suppressor mutations on vRNA replication. *E*, effect of the second site suppressor mutations of the second site suppressor mutants found for mutation D24A (depicted in shaded bars) on vRNA replication. All of the experiments and analysis were performed as described in the legend to Fig. 2. The values depicted in the graphs represent the means \pm S.E. of at least three independent experiments (*B*, *D*, and *E*) or at least four independent experiments (*C*). *c*, significantly different from 3A-D24A ($p < 0.05$); *d*, significantly different from 3A-D24A/K41N ($p < 0.05$); *e*, significantly different from 3A-D24A/K41Q ($p < 0.05$). *WB*, Western blot.

Structure-Function Analysis of CVB3 3A

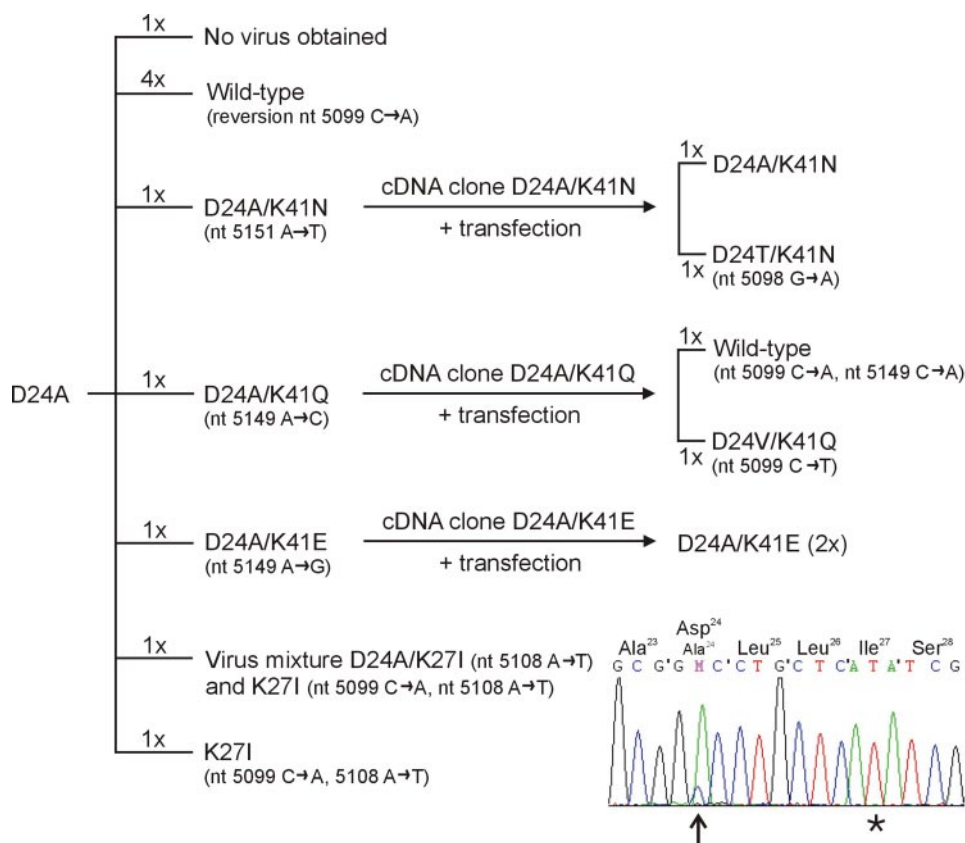


FIGURE 4. Identification of second site suppressor mutations for mutation D24A. Ten transfections were performed with RNA transcribed from the cDNA clone containing mutation D24A. The 3A sequence of the obtained viruses is shown. The mutations D24A/K41N, D24A/K41Q, and D24A/K41E were introduced into the cDNA clone, and the result of transfections with RNA transcribed from these clones is depicted. The nucleotide changes leading to the amino acid substitutions are indicated. The sequence plot of the virus mixture containing D24A/K27I and K27I is shown. The asterisk indicates the nucleotide change resulting in the K27I substitution. The arrow indicates the nucleotide that differs between the two populations of which the virus mixture is comprised (the major population contains an adenine residue resulting in Asp²⁴, whereas the minor part contains a cytosine residue resulting in Ala²⁴).

The quasi-infectious phenotype of mutation D24A is probably due to a primary defect in replication, because *in vitro* translation reactions showed no obvious defects in the polyprotein processing pattern (data not shown). Indeed, the replicon containing this mutation showed no detectable replication (Fig. 3D). The second site suppressor mutations K41N, K41Q, K41E, and K27I all significantly increased the level of vRNA replication compared with D24A ($p < 0.05$) (Fig. 3D), indicating that these mutations rescued virus growth by improving the function of 3A in vRNA replication. The observation that all second site suppressor mutations occurred at aa 27 or 41 suggests that a functional relationship exists between Asp²⁴, Lys²⁷, and Lys⁴¹.

We reasoned that the second site suppressor mutations for D24A might improve vRNA replication by improving dimerization of 3A. Therefore, dimerization levels of these mutants were tested (Fig. 3B). Mutations D24A/K41E and K27I, which restored replication to the highest levels, significantly improved dimerization compared with the D24A mutant ($p < 0.05$). However, no significant increases in dimerization were observed for mutations D24A/K41N, D24A/K41Q, and D24A/K27I, which restored replication to only low levels.

We also investigated whether these second site suppressor mutations restored the inhibition of protein transport (Fig. 3C).

Mutants D24A/K41E and K27I, which showed a strongly improved dimerization, were also more potent in inhibiting protein transport than the D24A mutant. The activities of these two second site suppressor mutants did not significantly differ from that of 3A wt. In contrast, the transport inhibiting activities of mutants D24A/K41N, D24A/K41Q, and D24A/K27I were only slightly increased compared with that of the D24A mutant and significantly differed from that of 3A wt. Together, these data point to a correlation between the level of 3A dimerization on the one hand and its activity in vRNA replication and ability to inhibit protein transport on the other hand.

To demonstrate that the observed growth of mutant viruses is caused by aa changes at position 41 of 3A and not by possible other mutations in a part of the virus that was not sequenced, mutations D24A/K41N, D24A/K41Q, and D24A/K41E were introduced into the infectious cDNA clone. BGM cells were transfected with copy RNA transcripts of these mutants in duplicate and showed virus growth on both occasions for all mutants (Fig. 4). Sequence analysis of the obtained virus populations showed

that upon transfection of RNA carrying mutations D24A/K41N, the mutations were retained in one case, whereas in the other case the residue at position 24 was substituted for a Thr (D24T/K41N). Upon transfection of RNA carrying mutations D24A/K41Q, the K41Q mutation was retained, but a Ala-to-Val substitution at aa 24 had occurred in one case (D24V/K41Q), whereas in the other case both mutations had reverted back to wt. Upon transfection of RNA carrying mutations D24A/K41E, both mutations were retained in both cases. We reasoned that the newly found second site suppressor mutations might further improve replication as compared with their ancestors. Hence, we introduced the newly found mutations into the subgenomic replicon. Indeed, mutation D24T/K41N significantly improved replication as compared with its ancestor D24A/K41N ($p < 0.05$) (Fig. 3E). Similarly, mutation D24V/K41Q significantly improved replication as compared with D24A/K41Q ($p < 0.05$) (Fig. 3E). Thus, the second site suppressor mutations K41N, K41Q, and K41E indeed rescued the defect in virus growth caused by mutation D24A.

Investigation of the Biological Significance of Ser²⁸ and Tyr³⁷—The molecular model of CVB3 3A predicts an intermolecular hydrogen bond between Ser²⁸ and Tyr³⁷ (Fig. 5A). All of the enteroviruses sequenced to date contain a Tyr at position 37 (Fig.

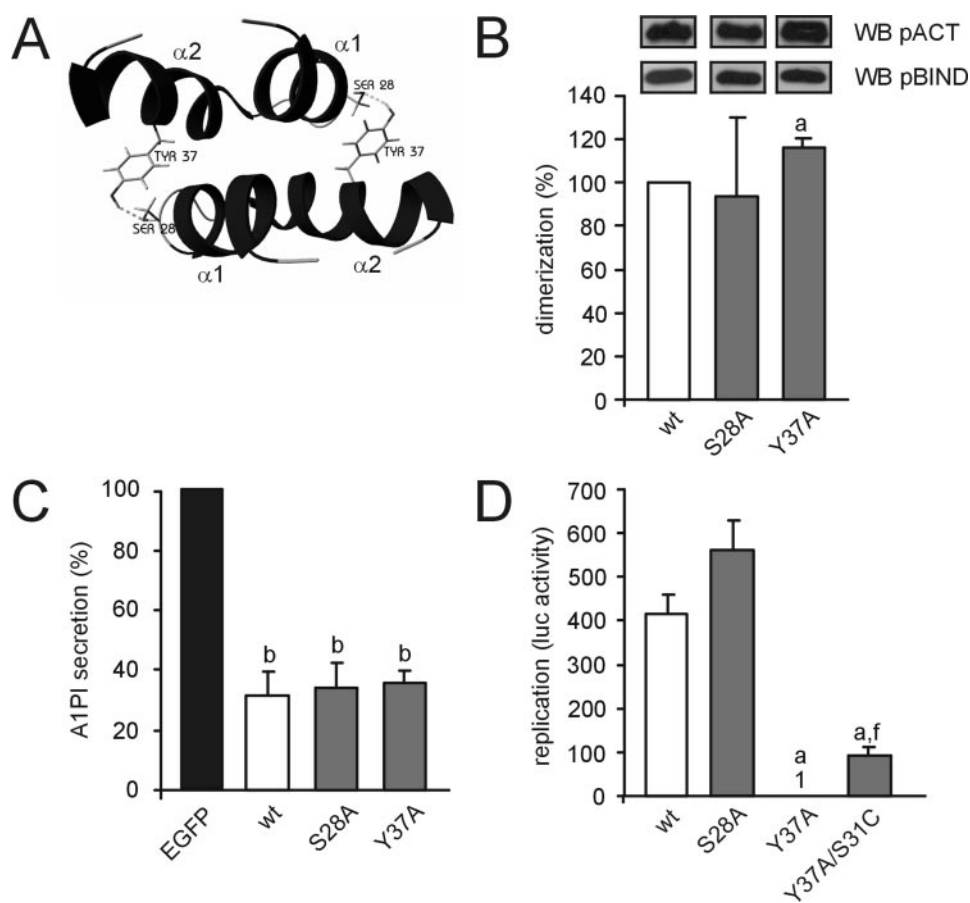


FIGURE 5. Ser²⁸ and Tyr³⁷ are not important for dimerization of 3A. *A*, structural model of the predicted intermolecular hydrogen bond between Ser²⁸ and Tyr³⁷. *B*, effect of mutations S28A and Y37A on 3A dimerization. *C*, effect of mutations S28A and Y37A on the ability of 3A to inhibit protein transport. *D*, effect of mutations S28A and Y37A on vRNA replication. All of the experiments and analysis were performed as described in the legend to Fig. 2. The values depicted in the graphs of *B–D* represent the means \pm S.E. of at least three independent experiments. *f*, significantly different from 3A-Y37A ($p < 0.05$). *WB*, Western blot.

1B). Ser²⁸ is conserved among the HEV-B and HEV-D members, but not among PV and some HEV-C members, which contain an Ala at the corresponding position (Fig. 1C). Mutants S28A and Y37A were both capable of dimerization (Fig. 5B) and were not affected in their ability to inhibit protein secretion (Fig. 5C). Cells transfected with RNA transcripts of the infectious cDNA clone containing mutation S28A exhibited virus growth in all cases, and sequence analysis showed that the mutation was retained. As expected, mutation S28A had no effect on the level of replication (Fig. 5D). Cells transfected with transcripts containing mutation Y37A exhibited virus growth in one of four cases. Sequence analysis showed that the introduced mutation was retained in the obtained virus but that a Ser-to-Cys substitution at aa 31 (nucleotide 5119, A \rightarrow T) had occurred. The Y37A mutant showed no detectable replication, but the second site suppressor mutation S31C partially restored the replication. These data suggest that residues Ser²⁸ and Tyr³⁷ are not required for efficient dimerization. Ser²⁸ is not essential for any of the functions of 3A tested in this study, whereas Tyr³⁷ is essential for vRNA replication, but not for inhibition of protein transport.

A Conserved N-terminal Domain Is Important for the Ability of 3A to Inhibit Protein Transport—Almost all enteroviruses (excluding HEV-A viruses and one HEV-C member) contain at positions 6–10 positive charged, negative charged, hydropho-

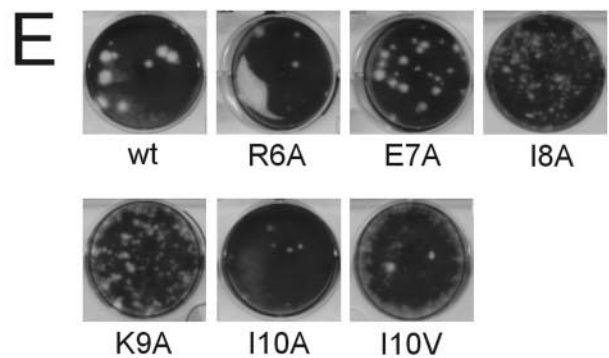
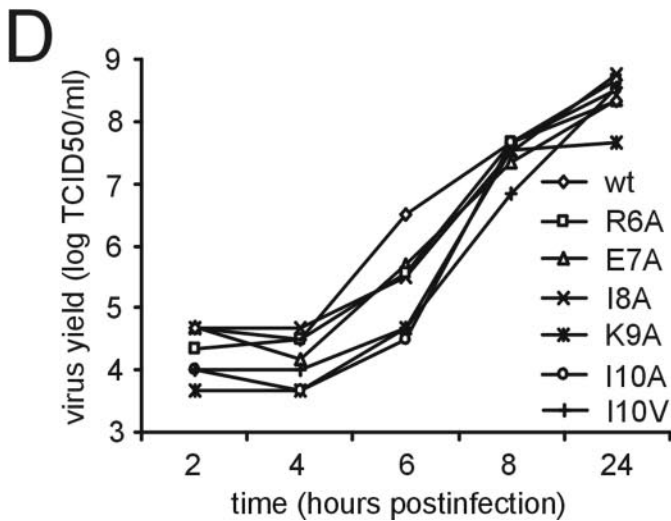
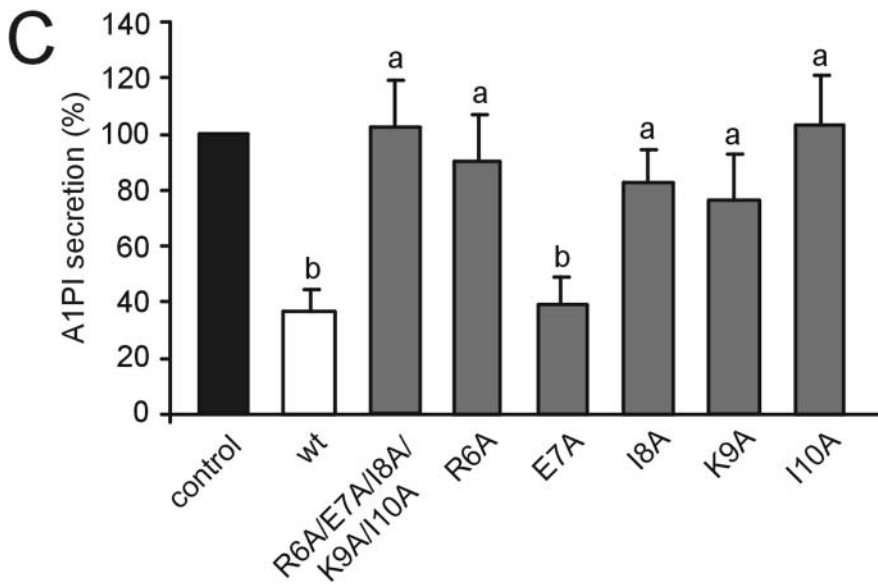
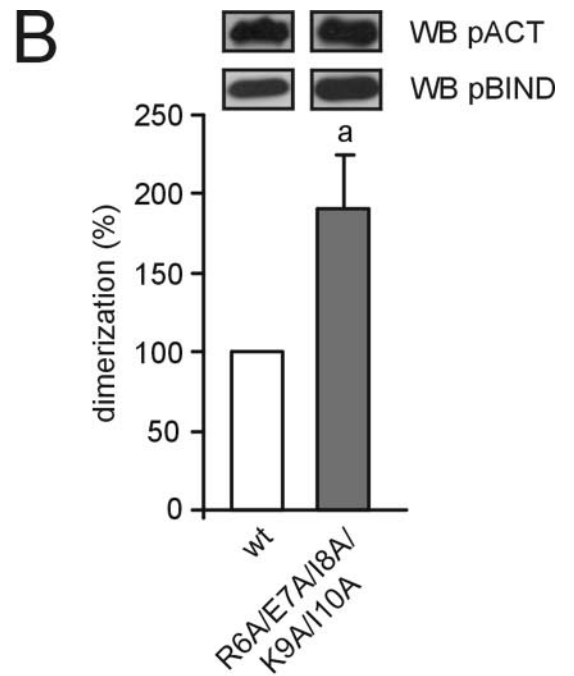
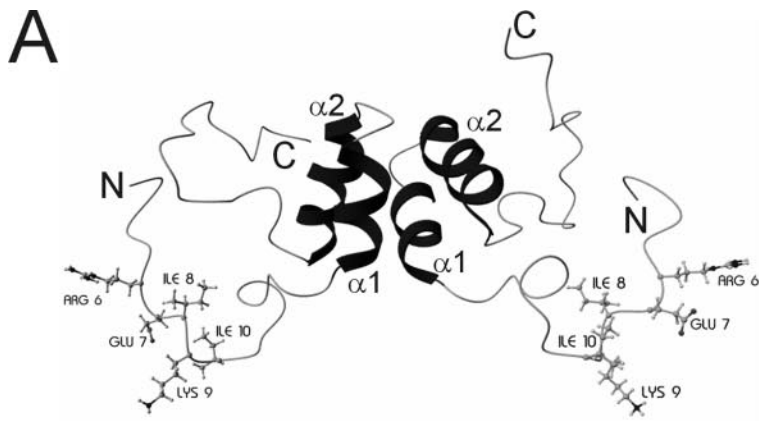
bic, positive charged, and Ile residues, respectively (Figs. 1B and 6A). We called these residues the conserved N-terminal domain (CND). The N-terminal 19 aa of the 3A protein, in which this CND resides, were predicted to form an unstructured region, and this region was not implicated in dimer formation of the 3A protein. Indeed, mutation of the CND did not disturb the ability of 3A to form homodimers (Fig. 6B). Thus, conservation of these residues points to their importance for another function of the 3A protein.

We also studied whether the CND mutant could inhibit protein transport and support vRNA replication. A mutant in which the five residues of the CND were substituted for Ala residues was not able to inhibit protein secretion (Fig. 6C). To study the role of the CND in inhibition of protein transport in further detail, mutant proteins were generated in which single residues of the CND were substituted for Ala residues. Except mutation E7A, all single amino substitutions significantly decreased the ability of 3A to inhibit protein transport ($p < 0.05$) (Fig. 6C).

No virus growth was observed upon transfection of RNA transcripts in which all five residues of the CND were mutated. *In vitro* translation reactions showed no obvious defects in the polyprotein processing pattern, making this an unlikely cause for the lack of virus growth (data not shown). We also studied the effect of single alanine substitutions within the CND on virus viability. Transfection of RNA transcripts carrying these single mutations resulted in virus growth in all cases. Sequence analysis of the obtained viruses showed that the introduced mutations were retained in the vRNA in all cases with mutations R6A, E7A, I8A, and K9A and in one case with mutation I10A. In the other three cases of mutation I10A, an Ala-to-Val substitution at aa 10 (nucleotide 5060, C \rightarrow T) had occurred. All of the viruses containing mutations R6A, E7A, I8A, K9A, I10A, or I10V showed efficient replication but were slightly impaired in growth compared with the wt virus, as indicated by a delay in replication in a single cycle growth analysis (Fig. 6D) and a smaller plaque phenotype (Fig. 6E). Together, our data show that single residues in the CND are essential for inhibition of protein transport but not for dimerization or virus growth.

DISCUSSION

In this paper, we described a structure-function analysis of the CVB3 3A protein. Using the NMR structure of the related PV 3A as a template (20), we derived a molecular model for the



N-terminal 60 aa of CVB3 3A. The model shows that 3A contains two α -helices (aa 20–27 and 31–42) that form a helical hairpin, whereas the remaining N- and C-terminal tails seem to be unstructured. Like PV 3A, CVB 3A is able to form homodimers. Based on the model and on sequence conservation among the enteroviruses, we identified several possible determinants for the formation of these homodimers: (i) a hydrophobic interaction between the helical hairpins of both monomers, (ii) an intermolecular salt bridge between Asp²⁴ and Lys⁴¹, and (iii) an intermolecular hydrogen bond between Ser²⁸ and Tyr³⁷. We substituted individual residues that were conserved or were predicted to play a role in dimerization by Ala residues to investigate their importance for the function of the 3A protein. Using this approach, we showed that dimerization is important for efficient virus replication and inhibition of protein transport. When dimerization is disturbed, *e.g.* by substituting residues that participate in the predicted hydrophobic interaction (Leu²⁵ and Leu²⁶) or in the predicted salt bridge (Asp²⁴), replication is reduced to background levels, and the ability of 3A to inhibit protein transport is lost.

Upon mutation of Asp²⁴ to Ala (D24A), a number of viruses were isolated carrying second site suppressor mutations that (partially) restored the function of 3A. All of the second site suppressor mutations occurred at residues Lys²⁷ and Lys⁴¹, suggesting that residues at positions 24, 27, and 41 are functionally linked. When the negatively charged Asp²⁴ is substituted by an apolar Ala, both the intermolecular (Asp²⁴–Lys⁴¹) and intramolecular (Asp²⁴–Lys²⁷) salt bridges are lost. Second site suppressor mutations in which the positively charged Lys⁴¹ is replaced for a polar residue (Asn and Gln) or a negatively charged residue (Glu) can compensate for this. The positive charges of Lys²⁷ and Lys⁴¹ are located close to each other in the 3A dimer, and the repulsion between these positive charges is diminished by their interaction with the negatively charged Asp²⁴. When the negative charge of Asp²⁴ is lost, repulsion between Lys²⁷ and Lys⁴¹ can no longer be compensated. It might be that the second site suppressors compensate the positive charges of Lys²⁷ and Lys⁴¹ and thereby diminish their electrostatic repulsion. Alternatively or in addition, the negatively charged or polar residues may form an intermolecular salt bridge or hydrogen bond with Lys²⁷, respectively.

Our experimental data show a higher level of dimerization for the D24A/K41E mutant as compared with the D24A/K41N and D24A/K41Q mutants. This might reflect the strength of the chemical bond between residues 27 and 41 (the Lys²⁷–Glu⁴¹ salt bridge is a stronger chemical bond than the Lys²⁷–Asn⁴¹ and Lys²⁷–Gln⁴¹ hydrogen bonds) or the extent in which the electrostatic repulsion between Lys²⁷ and Lys⁴¹ is compensated. In a second series of suppressor mutations that were

found after RNA transfection of mutants D24A/K41N and D24A/K41Q, the introduced Ala²⁴ was substituted by Thr or Val residues (D24T/K41N and D24V/K41Q, respectively). These Thr or Val residues at position 24 may further contribute to dimerization by strengthening the hydrophobic interaction between the helical hairpins.

In addition to second site suppressor mutations at position 41, a suppressor mutation at position 27 was identified (K27I). In one occasion, transfection of RNA carrying mutation D24A gave rise to a K27I containing virus mixture in which the introduced D24A mutation was still present in a minor part of the population, whereas in the major part of the population the introduced D24A mutation had reverted to wt. It is tempting to speculate that the K27I virus had a growth advantage over the D24A/K27I virus and thereby became the dominant species within this mixture. This idea is supported by the higher vRNA replication level of K27I compared with D24A/K27I. How can a Lys-to-Ile substitution at position 27 rescue the adverse effect of the D24A mutation? The electrostatic repulsion that arises between Lys²⁷ and Lys⁴¹ upon the loss of the compensating negative charge of Asp²⁴ may be counteracted by substitution of Lys²⁷ for a residue lacking this positive charge. In addition, Ile has a large hydrophobic side chain that may further contribute to the hydrophobic interaction between the helical hairpins. Taken together, our results support a model in which an intermolecular salt bridge contributes to dimerization.

A correlation was observed between the efficiency of dimerization on the one hand and the activity of 3A in vRNA replication and transport inhibition on the other hand. Mutations D24A/K41N, D24A/K41Q, and D24A/K27I, for which little, if any, increase in dimerization could be observed (which may be due to the limited sensitivity of the assay used), rescued vRNA replication and transport inhibition to only low levels. Mutations D24A/K41E and K27I (without D24A), which significantly improved dimerization, rendered 3A more active in transport inhibition. Mutation K27I also restored vRNA replication to the wild type level. The finding that mutation D24A/K41E, which improved dimerization and transport inhibition to similar levels as K27I, restored vRNA replication to only ~25% of wild type level shows that, in addition to dimerization, sequence-specific determinants influence the efficiency of vRNA replication.

Mutations targeted to the CND, which is of major importance for the inhibition of protein transport, did not decrease dimerization. Instead, an increased dimerization efficiency was observed. The reason for this is unknown. Dimerization efficiency may be affected by primary sequence features of the CND or, alternatively, by proteins that may bind to this conserved motif. Alanine substitutions of individual resi-

FIGURE 6. A CND, which is not important for 3A dimerization, is required for inhibition of protein transport by 3A. *A*, structural model of the N-terminal 60 aa of CVB3 3A, in which aa 6–10 (Arg, Glu, Ile, Lys, and Ile) are indicated. *B*, effect of CND mutation on 3A dimerization. *C*, effect of CND mutation on the ability of 3A to inhibit protein transport. All of the experiments and analysis were performed as described in the legend to Fig. 2. The values depicted in the graphs of *B* and *C* represent the means \pm S.E. of at least three independent experiments. *D* and *E*, effect of CND mutations on virus growth, depicted by single-cycle growth analysis (*D*) and plaque assays (*E*). For the single-cycle growth analysis, BGM cells were infected at a multiplicity of infection of 5, incubated at 37 °C, and harvested at 2, 4, 6, 8, or 24 h post-infection. The viruses were released by three cycles of freezing and thawing, and virus titers were determined by end-point titration on BGM cells and expressed in TCID₅₀/ml values. For the plaque assays, BGM cells were infected with serial dilutions of CVB3 wt or mutants. At 30 min post-infection, the virus was replaced for M199 medium containing 0.5% agarose. The cells were incubated at 37 °C for 2 days and stained with crystal violet. *WB*, Western blot.

Structure-Function Analysis of CVB3 3A

dues in this region resulted in viruses that showed slightly impaired growth characteristics. However, the ability to inhibit protein transport was completely lost upon substitution of Arg⁶, Ile⁸, Lys⁹, or Ile¹⁰ of the CND. An important role for Lys⁹ in inhibition of protein transport was also described for the 3A proteins of PV and the closely related human rhinovirus 14 (29). In contrast to the residues at positions 6, 8, 9, and 10, the residue at position 7 is not conserved and is a Pro in HEV-A viruses, whereas it is an acid residue in the other enterovirus species. Indeed, we found that Glu⁷ was not essential for ability of 3A to inhibit protein transport. Thus, in addition to dimerization, sequence conservation and residue identity in the CND is also essential for inhibition of secretion. For this function, it is very likely that a cellular protein involved in secretory pathway transport interacts with the 3A dimer. We propose a model in which dimerization creates a binding pocket for this cellular counterpart, which is defined by the CNDs of both 3A monomers.

Upon substitution of individual residues of the CND, viruses were obtained that grew efficiently, although with slightly impaired growth characteristics. Alanine substitutions of most of these residues drastically disturbed the ability to inhibit protein transport. These results confirm that the inhibition of protein transport is not essential for vRNA replication, as has been demonstrated earlier (4, 5). However, the finding that growth of viruses carrying single mutations in the CND is slightly affected leaves open the possibility that the 3A-mediated inhibition of protein transport may contribute to some extent to vRNA replication.

Using mutational analysis, we confirmed that residues involved in the predicted hydrophobic interaction and salt bridge are important for dimerization, replication, and inhibition of transport. In contrast, substitution of Ser²⁸ and Tyr³⁷, which were predicted to form an intermolecular hydrogen bond, did not influence dimerization or inhibition of secretion. Therefore, it is very likely that the predicted hydrogen bond, if formed at all, does not contribute to dimerization. Ser²⁸ is not conserved among enteroviruses; it is not present in PV 3A, nor can an equivalent hydrogen bond be formed in the PV dimer. In contrast to Ser²⁸, Tyr³⁷ is conserved among enteroviruses. In the PV structure, the corresponding Tyr was assigned as part of the hydrophobic surface of the helical hairpin (20) and thus would contribute to dimerization. However, when we mutated this residue in CVB3 3A, dimerization still occurred with wt efficiency, and protein transport was inhibited to the same levels as seen for wt 3A. In sharp contrast, viral replication was reduced to background levels. These observations indicate that Tyr³⁷ plays an important role in vRNA replication, possibly by forming a contact site for a viral or cellular protein.

The defect in vRNA replication induced by the Y37A mutation was found to be rescued by the second site suppressor mutation S31C. Remarkably, this same second site suppressor mutation was previously identified to rescue the defect in vRNA replication caused by mutations P17A/P18A/P19A in 3A (5). Introduction of the S31C mutation in wt 3A reduced vRNA replication (data not shown), whereas it increased vRNA replication in the Y37A and P17A/P18A/P19A mutants. We generated a model of the 3A S31C

mutant, and in this model the Cys³¹ residues were predicted to be close to each other (data not shown). Thus, it is possible that an intermolecular disulfide bond is formed that contributes to dimerization. This possibility cannot be excluded, but the Y37A mutant already dimerized with wt efficiency, making it unlikely that an increase in dimerization is needed to rescue the growth defect caused by this mutation. How the S31C suppressor mutation can (partially) rescue the defect in vRNA replication remains to be established.

Are the determinants for CVB3 3A dimerization that we identified in this study conserved in PV? To gain more insight into the determinants for PV 3A dimerization, we optimized the published PV 3A structure using the YASARA NOVA force field package and validated it by WHAT_CHECK (data not shown). The hydrophobic interaction between the helical hairpins of both monomers was predicted for PV (20) and was also visible in our optimized PV 3A model. In addition, an intermolecular salt bridge between Asp²³ and Lys⁴⁰ (which correspond to Asp²⁴ and Lys⁴¹ in CVB3 3A) was predicted (data not shown). Thus, the determinants that we experimentally showed to contribute to CVB3 3A dimerization, seem to be conserved in PV 3A. A remarkable difference between PV and CVB3 3A is an intermolecular disulfide bond at Cys²⁰, which is predicted in our optimized PV model but cannot be formed in the CVB3 model, because it lacks the corresponding Cys residue (data not shown). There is no experimental data supporting the presence of this disulfide bond in the PV 3A dimer. Hence, it is unclear whether this difference between the PV and CVB3 dimer indeed exists.

In conclusion, we showed that 3A dimerization is important for both efficient inhibition of protein transport and efficient support of vRNA replication. We identified two types of interactions that contributed to dimerization, namely a hydrophobic interaction between the helical hairpins of the individual monomers and an intermolecular salt bridge. Furthermore, a domain was identified in the unstructured N terminus that plays an important role in inhibition of protein secretion. The combination of *in vivo* and *in silico* results obtained in this study provide important insights in both structural and functional aspects of 3A. Future studies on dimerization and interactions of 3A with other viral proteins and cellular binding partners may benefit from the dimer model that we present here.

REFERENCES

1. Porter, A. G. (1993) *J. Virol.* **67**, 6917–6921
2. Wimmer, E., Hellen, C. U., and Cao, X. (1993) *Annu. Rev. Genet.* **27**, 353–436
3. Doedens, J. R., and Kirkegaard, K. (1995) *EMBO J.* **14**, 894–907
4. Doedens, J. R., Giddings, T. H., Jr., and Kirkegaard, K. (1997) *J. Virol.* **71**, 9054–9064
5. Wessels, E., Duijsings, D., Notebaart, R. A., Melchers, W. J., and van Kuppeveld F. J. (2005) *J. Virol.* **79**, 5163–5173
6. Dodd, D. A., Giddings, T. H., Jr., and Kirkegaard, K. (2001) *J. Virol.* **75**, 8158–8165
7. Deitz, S. B., Dodd, D. A., Cooper, S., Parham, P., and Kirkegaard, K. (2000) *Proc. Natl. Acad. Sci. U. S. A.* **97**, 13790–13795
8. Neznanov, N., Kondratova, A., Chumakov, K. M., Angres, B., Zhumabayeva, B., Agol, V. I., and Gudkov, A. V. (2001) *J. Virol.* **75**, 10409–10420
9. Bernstein, H. D., Sarnow, P., and Baltimore, D. (1986) *J. Virol.* **60**, 1040–1049

10. Giachetti, C., Hwang, S. S., and Semler, B. L. (1992) *J. Virol.* **66**, 6045–6057
11. Hope, D. A., Diamond, S. E., and Kirkegaard, K. (1997) *J. Virol.* **71**, 9490–9498
12. Xiang, W., Cuconati, A., Paul, A. V., Cao, X., and Wimmer, E. (1995) *RNA* **1**, 892–904
13. Paul, A. V., van Boom, J. H., Filippov, D., and Wimmer, E. (1998) *Nature* **393**, 280–284
14. Molla, A., Harris, K. S., Paul, A. V., Shin, S. H., Mugavero, J., and Wimmer, E. (1994) *J. Biol. Chem.* **269**, 27015–27020
15. Lama, J., Paul, A. V., Harris, K. S., and Wimmer, E. (1994) *J. Biol. Chem.* **269**, 66–70
16. Paul, A. V., Cao, X., Harris, K. S., Lama, J., and Wimmer, E. (1994) *J. Biol. Chem.* **269**, 29173–29181
17. Harris, K. S., Xiang, W., Alexander, L., Lane, W. S., Paul, A. V., and Wimmer, E. (1994) *J. Biol. Chem.* **269**, 27004–27014
18. Lyle, J. M., Bullitt, E., Bienz, K., and Kirkegaard, K. (2002) *Science* **296**, 2218–2222
19. Towner, J. S., Ho, T. V., and Semler, B. L. (1996) *J. Biol. Chem.* **271**, 26810–26818
20. Strauss, D. M., Glustrom, L. W., and Wuttke, D. S. (2003) *J. Mol. Biol.* **330**, 225–234
21. Van Ooij, M. J. M., Vogt, D. A., Paul, A., Castro, C., Kuijpers, J., van Kuppeveld, F. J. M., Cameron, C. E., Wimmer, E., Andino, R., and Melchers, W. J. G. (2006) *J. Gen. Virol.* **87**, 103–113
22. de Jong, A. S., Schrama, I. W., Willems, P. M., Galama, J. M., Melchers, W. J., and van Kuppeveld, F. J. (2002) *J. Gen. Virol.* **83**, 783–793
23. van Kuppeveld, F. J. M., Galama, J. M. D., Zoll, J., and Melchers, W. J. G. (1995) *J. Virol.* **69**, 7782–7790
24. van Ooij, M. J. M., Glaudemans, H. R. F., Heus, H. A., van Kuppeveld, F. J. M., and Melchers, W. J. G. (2006) *J. Gen. Virol.* **87**, 689–695
25. Vriend, G. (1990) *Mol. Graph.* **8**, 52–56
26. Chinea, G., Padron, G., Hooft, R. W., Sander, C., and Vriend, G. (1995) *Proteins* **23**, 415–421
27. Krieger, E., Koraimann, G., and Vriend, G. (2002) *Proteins* **47**, 393–402
28. Hooft, R. W. W., Vriend, G., Sander, G., and Abola, E. E. (1996) *Nature* **381**, 272
29. Choe, S. S., Dodd, D. A., and Kirkegaard, K. (2005) *Virology* **337**, 18–29